Iron−Semiquinone, Semiquinone−Semiquinone, and Iron−Iron Magnetic Exchange in Monomeric and Dimeric Ferric Complexes Containing the 3,6-Di-*tert*-butyl-1,2-semiquinonate Ligand

Attia S. Attia,† Brenda J. Conklin, Christopher W. Lange, and Cortlandt G. Pierpont*

Department of Chemistry and Biochemistry, University of Colorado, Boulder, Colorado 80309

Received May 16, 1995[⊗]

$Fe(3,6\text{-}DBSQ)_3$ has been prepared by reacting 3,6-di-*tert*-butyl-1,2-benzoquinone with $Fe(CO)_5$. The complex has been characterized structurally [orthorhombic, *Pbca*, $a = 18.277(5)$ Å, $b = 11.634(3)$ Å, $c = 39.903(10)$ Å, $V = 8485(4)$ Å^3, $Z = 8$, $R = 0.063$], electrochemically, and magnetically. Ligand-based redox couples are observed in electrochemical experiments that consist of reversible or quasireversible Cat/SQ steps at negative potentials and irreversible SQ/BQ oxidations at positive potentials. Magnetic measurements show temperature dependence that arises from antiferromagnetic exchange. Data have been fit to an expression that includes the effects of both Fe−SQ and SQ−SQ exchange with the result that J_{SQ-SQ} is larger in magnitude than J_{Fe-SQ}. In methanol, the complex undergoes solvolysis to form $[Fe(3,6\text{-}DBSQ)_2(\mu\text{-}OMe)]_2$. Structural characterization [triclinic, $P\bar{1}$, $a = 11.441(2)$ Å, $b = 11.514(2)$ Å, $c = 14.552(2)$ Å, $\alpha = 67.86(1)°$, $\beta = 70.51(1)°$, $\gamma = 72.79(1)°$, $V = 1641.8(5)$ Å^3, $Z = 1$, $R = 0.048$] has shown that the molecule is a centrosymmetric dimer with no close intermolecular contacts. The temperature dependence of magnetic measurements has been fit to a model consisting of two interacting $S = {}^3/_2$ centers that arise from strong Fe−SQ exchange with $J_{Fe-Fe} = -22.4$ cm^{-1}.

Introduction

1,2-Semiquinone complexes of iron were among the earliest radical semiquinone complexes of the transition metals.[1−3] A difficulty with characterization on quinone complexes of paramagnetic metal ions is the definition of charge distribution between ligand and metal. Mossbauer spectra recorded on the tris(quinone) complexes of iron showed clearly that the metal center was high-spin Fe(III), leading to the $Fe^{III}(SQ)_3$ formulation for products obtained from reactions carried out with $Fe(CO)_5$ and an appropriate 1,2-benzoquinone.[4−6] Two features of these compounds have been addressed in the present investigation. Because these complexes consist of paramagnetic radical ligands chelated with $S = {}^5/_2$ Fe(III), the temperature dependence of their magnetic properties is of interest with respect to contributions from both Fe−SQ and SQ−SQ spin-coupling interactions. Secondly, as the complexes consist of redox-active ligands, multistep electrochemical activity may be anticipated that involves both the metal and ligands. Complexes of iron have been studied with a variety of semiquinones that include ligands derived from tetrachloro-1,2-benzoquinone, 9,10-phenanthrenequinone, and 3,5-di-*tert*-butyl-1,2-benzoquinone.[1,4,5] Reactions carried out with 3,5-DBBQ are complicated by the formation of oligomeric products that result from bi- and trimetallic bridging interactions with the oxygen atom at the rings 1-position.[5] Tetrameric $[Fe^{III}(3,5\text{-}DBSQ)(3,5\text{-}DBCat)]_4$ (**I**),formed as a coproduct with $Fe(3,5\text{-}DBSQ)_3$ in the reaction of $Fe(CO)_5$ and 3,5-DBBQ, is a specific illustration of

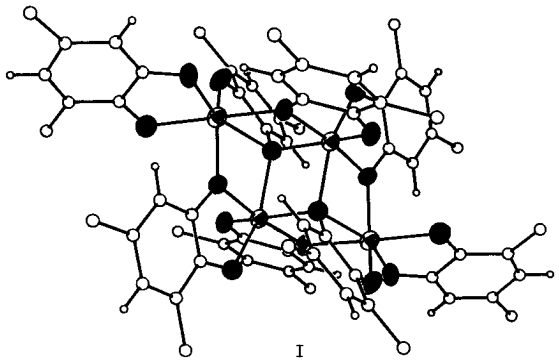

I

the difficulty with product separation and identification in reactions carried out with 3,5-DBBQ. In more recent syntheses, we have used 3,6-DBBQ to avoid these difficulties. Bulky *tert*-butyl substituents adjacent to both oxygen atoms block bridging interactions with nonchelated metal ions, and only products containing chelated quinone ligands are obtained. We now describe the synthesis and characterization of $Fe(3,6\text{-}DBSQ)_3$. This compound has been of specific interest as a precursor to the $Fe^{III}(N\text{-}N)(3,6\text{-}DBSQ)(3,6\text{-}DBCat)$ complexes by addition of bpy, tmeda, or pyridine ligands in studies on the potential for formation of $Fe^{III}(Cat)$ and $Fe^{II}(SQ)$ redox isomers.[7,8] In methanol solution, $Fe(3,6\text{-}DBSQ)_3$ has been observed to undergo solvolysis, and the dimeric product of this reaction, $[Fe(3,6\text{-}DBSQ)_2(\mu\text{-}OMe)]_2$, has been obtained in crystalline form. It represents a new addition to the quinone coordination chemistry of iron, and as a complex consisting of radical ligands chelated to bridged high-spin metal ions, it offers an opportunity for study of potentially complicated magnetic behavior that may result from the combined effects of Fe−SQ, SQ−SQ, and Fe−Fe exchange.

† Present address: Ain Shams University, Cairo, Egypt.

⊗ Abstract published in *Advance ACS Abstracts,* February 1, 1996.

(1) Buchanan, R. M.; Downs, H. H.; Shorthill, W. B.; Pierpont, C. G.; Kessel, S. L.; Hendrickson, D. N. *J. Am. Chem. Soc.* **1978**, *100*, 4318.
(2) Pierpont, C. G.; Buchanan, R. M. *Coord. Chem. Rev.* **1981**, *38*, 45.
(3) Pierpont, C. G.; Lange, C. W. *Prog. Inorg. Chem.* **1993**, *41*, 381.
(4) Buchanan, R. M.; Kessel, S. L.; Downs, H. H.; Pierpont, C. G.; Hendrickson, D. N. *J. Am. Chem. Soc.* **1978**, *100*, 7894.
(5) Boone, S. R.; Purser, G. H.; Chang, H.-R.; Lowery, M. D.; Hendrickson, D. N.; Pierpont, C. G. *J. Am. Chem. Soc.* **1989**, *111*, 2292.
(6) Cohn, M. J.; Xie, C.-L.; Tuchagues, J.-P. M.; Pierpont, C. G.; Hendrickson, D. N. *Inorg. Chem.* **1992**, *31*, 5028.
(7) Attia, A. S.; Jung, O.-S.; Pierpont, C. G. *Inorg. Chim. Acta* **1994**, *226*, 91.
(8) Attia, A. S.; Bhattacharya, S.; Pierpont, C. G. *Inorg. Chem.* **1995**, *34*, 4427.

0020-1669/96/1335-1033$12.00/0

Table 1. Crystallographic Data for $Fe(3,6\text{-DBSQ})_3$ and $[Fe(3,6\text{-DBSQ})_2(\mu\text{-OMe})]_2$

	$Fe(3,6\text{-DBSQ})_3$	$[Fe(3,6\text{-DBSQ})_2(\mu\text{-OMe})]_2$
formula	$C_{42}H_{60}O_6Fe$	$C_{62}H_{86}O_{10}Fe_2$
fw	716.8	1103.0
color	dark green	dark blue
space group	*Pbca*	$P\bar{1}$
a (Å)	18.277(5)	11.441(2)
b (Å)	11.634(3)	11.514(2)
c (Å)	39.903(10)	14.552(2)
α (deg)	90.0	67.86(1)
β (deg)	90.0	70.51(1)
γ (deg)	90.0	72.79(1)
V (Å^3)	8485(4)	3671(1)
Z	8	1
T (°C)	24−26	24−26
λ(Mo Kα) (Å)	0.710 73	0.710 73
D_{calcd} (g cm^{-3})	1.122	1.116
μ (mm^{-1})	0.393	0.488
R, R_w[a]	0.063, 0.082	0.048, 0.055

[a] $R = \sum||F_o| - |F_c||\sum|F_o|$; $R_w = [\sum w(|F_o| - |F_c|)^2/\sum w(F_o)^2]^{1/2}$.

Experimental Section

Materials. Iron pentacarbonyl was purchased from Strem Chemical Co. 3,6-Di-*tert*-butyl-1,2-benzoquinone (3,6-DBBQ) was prepared using a literature procedure.[9]

Complex Syntheses. Fe(3,6-DBSQ)$_3$. $Fe(CO)_5$ (0.3 mL, 2.3 mmol) and 3,6-DBBQ (0.17 g, 0.8 mmol) were dissolved in thf (50 mL). As the mixture was irradiated with a sun lamp (8 h), the color of the solution became dark green. Solvent was removed under vacuum, and the residue was dissolved in dichloromethane. Chromatographic separation on a silica gel column eluted with a CH_2Cl_2/hexane mixture gave $Fe(3,6\text{-DBSQ})_3$ as a green band. The product was isolated and recrystallized from hexane with 80% yield. Anal. Calc for $C_{42}H_{60}O_6Fe$: C, 70.3; H, 8.4. Found: C, 70.6; H, 7.9. UV−vis: 290 nm (5.7×10^4 M^{-1} cm^{-1}), 395 (1.5×10^4), 640 (1.6×10^4).

[Fe(*μ*-OMe)(3,6-DBSQ)$_2$]$_2$. $Fe(3,6\text{-DBSQ})_3$ (0.22 g, 0.31 mmol) was dissolved in a 1:1 anisole−methanol solution. The color of the solution became deep blue, and slow evaporation of the solvent gave the dimeric product as dark blue crystals in 75% yield. Anal. Calc for $C_{31}H_{43}O_5Fe$: C, 67.5; H, 7.8. Found: C, 66.3; H, 7.5. UV−vis: 290 nm (1.8×10^4 M^{-1} cm^{-1}), 365 (6.2×10^3), 392 (sh), 635 (4.3×10^3).

Physical Measurements. Electronic spectra were recorded on a Perkin-Elmer Lambda 9 spectrophotometer. Magnetic measurements were made using a Quantum Design SQUID magnetometer at a field strength of 5 kG. Infrared spectra were recorded on a Perkin-Elmer 1600 FTIR with samples prepared as KBr pellets. Cyclic voltammograms were obtained with a Cypress CYSY-1 computer-controlled electroanalysis system. A Ag/Ag^+ reference electrode was used that consisted of a CH_3CN solution of $AgPF_6$ in contact with a silver wire placed in glass tubing with a Vycor frit at one end to allow ion transport. Tetrabutylammonium hexafluorophosphate was used as the supporting electrolyte, and the Fc/Fc^+ couple was used as an internal standard. With this experimental arrangement, the Fc/Fc^+ couple appeared at 0.192 V vs Ag/Ag^+ with $\Delta E = 130$ mV without correction for cell *iR* drop.

Crystallographic Structure Determinations. Fe(3,6-DBSQ)$_3$. Dark green prismatic crystals of the complex were obtained by recrystallization from a hexane/dichloromethane solution. Axial photographs indicated orthorhombic symmetry and the centered settings of 25 intense reflections with 2θ values between 18 and 28° gave the unit cell dimensions listed in Table 1. Data were collected by $\theta-2\theta$ scans within the angular range 3.0−45°. A Patterson map was used to determine the location of the Fe atom, and phases derived from the metal gave the positions of other atoms of the structure. ψ scans recorded at the conclusion of data collection indicated that the effects of absorption were negligible. Final cycles of refinement converged with discrepancy indices of $R = 0.063$ and $R_w = 0.082$. Selected atomic coordinates are listed in Table 2. Tables containing a full listing of atom positions, anisotropic displacement parameters, and hydrogen atom locations are available as Supporting Information.

Table 2. Selected Atomic Coordinates ($\times 10^4$) and Thermal Parameters (Å^2) for $Fe(3,6\text{-DBSQ})_3$

	x/*a*	*y*/*b*	*z*/*c*	*U*(eq)
Fe	9586(1)	1567(1)	3774(1)	55(1)
O1	9704(2)	62(3)	4016(1)	56(2)
O2	10265(2)	738(4)	3465(1)	62(2)
C1	10244(3)	−527(5)	3911(2)	51(3)
C2	10581(3)	−142(6)	3597(2)	54(3)
C3	11204(3)	−681(6)	3458(2)	53(3)
C4	11457(3)	−1605(6)	3633(2)	63(3)
C5	11122(4)	−2013(6)	3930(2)	67(3)
C6	10530(3)	−1526(6)	4079(2)	58(3)
O5	9839(2)	3013(3)	3519(1)	59(2)
O6	10414(2)	2222(4)	4048(1)	60(2)
C29	10393(3)	3580(5)	3628(2)	50(2)
C30	10710(3)	3134(5)	3935(2)	48(2)
C31	11323(3)	3690(6)	4089(2)	53(3)
C32	11574(3)	4633(6)	3926(2)	62(3)
C33	11257(4)	5041(6)	3625(2)	66(3)
C34	10687(3)	4548(6)	3465(2)	56(3)
O3	8696(2)	1485(3)	3495(1)	54(2)
O4	8852(2)	2318(3)	4071(1)	59(2)
C15	8204(3)	2184(5)	3582(2)	48(2)
C16	8294(3)	2686(5)	3915(2)	45(2)
C17	7811(4)	3536(5)	4048(2)	55(2)
C18	7239(4)	3793(6)	3839(2)	65(3)
C19	7136(3)	3328(6)	3524(2)	63(3)
C20	7600(3)	2545(6)	3376(2)	52(2)

Table 3. Selected Atomic coordinates ($\times 10^4$) and Thermal Parameters (Å^2) for $[Fe(3,6\text{-DBSQ})_2(\mu\text{-OMe})]_2$

	x/*a*	*y*/*b*	*z*/*c*	*U*(eq)
Fe	818(1)	528(1)	−1094(1)	38(1)
O1	1271(4)	27(4)	−2379(3)	49(3)
O2	2550(4)	−620(4)	−1071(4)	47(2)
C1	2420(7)	−520(6)	−2646(6)	41(4)
C2	3177(7)	−873(6)	−1911(6)	41(4)
C3	4481(6)	−1437(7)	−2139(6)	47(4)
C4	4945(7)	−1680(7)	−3051(6)	58(4)
C5	4199(8)	−1378(7)	−3755(6)	58(4)
C6	2958(7)	−807(7)	−3606(6)	50(4)
O3	1788(4)	1974(4)	−1747(3)	47(2)
O4	−435(4)	2008(4)	−1755(3)	45(2)
C15	1282(7)	3008(7)	−2318(5)	39(4)
C16	6(6)	3012(7)	−2348(5)	39(4)
C17	−653(7)	4105(7)	−3011(5)	44(4)
C18	−38(7)	5087(7)	−3537(5)	52(4)
C19	1198(8)	5056(7)	−3479(6)	60(5)
C20	1892(7)	4060(7)	−2912(5)	46(4)
O5	529(4)	480(4)	333(3)	40(2)
C29	1410(7)	646(8)	749(6)	60(4)

[Fe(*μ*-OMe)(3,6-DBSQ)$_2$]$_2$. Dark blue plates of the complex were obtained by recrystallization from a methanol/anisole solution. Axial photographs indicated only triclinic symmetry, and the centered settings of 25 intense reflections with 2θ values between 18 and 25° gave the unit cell dimensions listed in Table 1. Data were collected by $\theta-2\theta$ scans within the angular range 3.0−45°. A Patterson map was used to determine the location of the Fe atom, and phases derived from Fe gave the positions of other atoms of the structure. Final cycles of refinement converged with discrepancy indices of $R = 0.048$ and $R_w = 0.055$. Selected atomic coordinates are listed in Table 3. Tables containing a full listing of atom positions, anisotropic displacement parameters, and hydrogen atom locations are available as Supporting Information.

Results

The semiquinone complexes of iron have been of interest as molecules that show relatively strong metal−radical magnetic exchange. Electrochemical activity at both the metal and

(9) Belostotskaya, I. S.; Komissarova, N. L.; Dzhuaryan, E. V.; Ershov, V. V. *Izv. Akad. Nauk SSSR* **1972**, 1594.

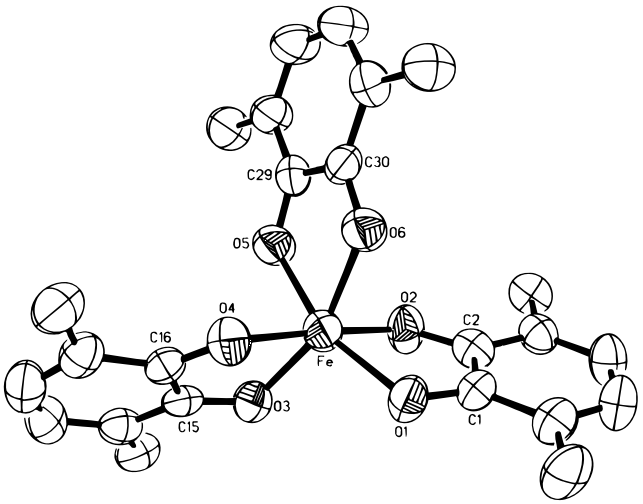

Figure 1. View of Fe(3,6-DBSQ)$_3$ with *tert*-butyl methyl carbon atoms omitted.

Table 4. Selected Bond Lenghts (Å) and Angles (deg) for Fe(3,6-DBSQ)$_3$

	Bond Lengths (Å)		
Fe−O1	2.010(4)	Fe−O2	1.999(4)
Fe−O3	1.975(4)	Fe−O4	1.991(4)
Fe−O5	2.022(4)	Fe−O6	2.016(4)
O1−C1	1.273(7)	O2−C2	1.287(8)
C1−C2	1.466(9)	C1−C6	1.440(9)
C2−C3	1.414(9)	C3−C4	1.365(9)
C4−C5	1.412(10)	C5−C6	1.359(9)
O3−C15	1.262(7)	O4−C16	1.270(7)
C15−C16	1.460(9)	C15−C20	1.440(9)
C16−C17	1.428(9)	C17−C18	1.371(9)
C18−C19	1.383(10)	C19−C20	1.378(9)
O5−C29	1.285(7)	O6−C30	1.273(8)
C29−C30	1.449(9)	C29−C34	1.408(9)
C30−C31	1.434(9)	C31−C32	1.356(9)
C32−C33	1.417(10)	C33−C34	1.349(9)
	Angles (deg)		
O1−Fe−O2	79.0(2)	O3−Fe−O4	78.7(2)
	O5−Fe−O6	77.7(2)	
(O1,O4,O6)−(O2,O3,O5) trigonal twist		43.1	

quinone ligands has been investigated for members of the Cr(SQ)$_3$ series[10] but not for the related complexes of iron. 3,6-Di-*tert*-butyl-1,2-benzoquinone reacts with Fe(CO)$_5$ to give Fe(3,6-DBSQ)$_3$. The structural, magnetic, and electrochemical properties of Fe(3,6-DBSQ)$_3$ and the methoxide-bridged dimer [Fe(3,6-DBSQ)$_2$(μ-OMe)]$_2$, formed by methanol solvolysis, are described herein.

Fe(3,6-DBSQ)$_3$. Structure. Crystals of Fe(3,6-DBSQ)$_3$ form in orthorhombic space group *Pbca* with no crystallographically imposed molecular symmetry. A view of the inner coordination geometry of Fe(3,6-DBSQ)$_3$ is shown in Figure 1; bond lengths and angles are listed in Table 4. Values for the Fe−O lengths are typical for Fe(III) but average to a value (2.002(4) Å) that is slightly shorter than the 2.027(4) and 2.015(2) Å lengths of Fe(PhenSQ)$_3$ and Fe(3,5-DBSQ)$_3$. Bond lengths within the three ligands show a pattern observed typically for chelated semiquinones. Carbon−oxygen lengths average to 1.275(7) Å, a value that is midway between the double-bond length of a benzoquinone and the single-bond length of a chelated catecholate, and a pattern of ring C−C

(10) Downs, H. H.; Buchanan, R. M.; Pierpont, C. G. *Inorg. Chem.* **1979**, *18*, 1736.

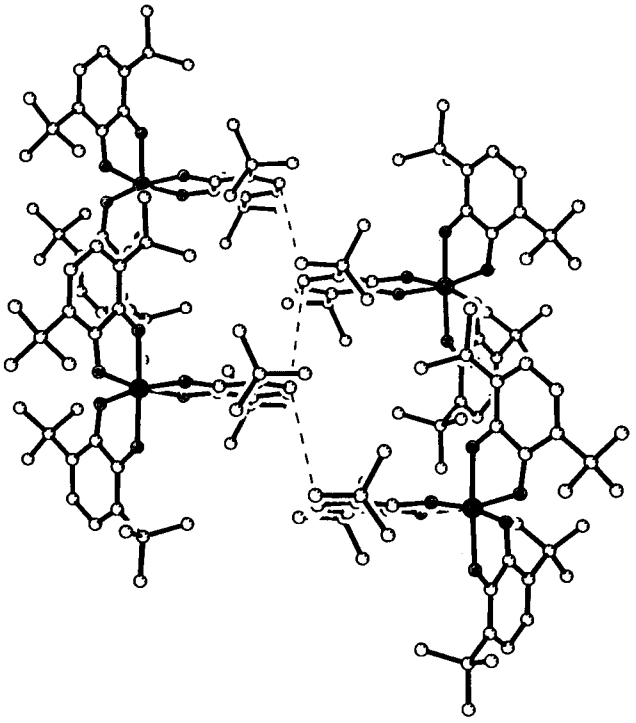

Figure 2. Closest intermolecular contacts between Fe(3,6-DBSQ)$_3$ molecules. Contacts between semiquinone C4 and C5 carbon atoms of adjacent complex molecules are 4.3−4.5 Å.

lengths that is slightly contracted at the C3−C4 and C5−C6 bond positions as a result of residual quinone double-bond localization. The crystal structure of Fe(3,6-DBSQ)$_3$ consists, in one view, of stacks of complex molecules with closest intermolecular contacts of 4.3 Å between the C4−C5 bonds of adjacent molecules (Figure 2) as the shortest intermolecular contact. Much of the semiquinone radical spin density is concentrated at this bond position, and intermolecular stacking may be responsible for low-temperature anomalies in the magnetic properties of the complex in the solid state.

Electrochemistry. The three semiquinone ligands of Fe(3,6-DBSQ)$_3$ offer the possibility for significant ligand-based redox activity. Scanning positively, CV's the complex show two sets of three oxidations from the [Fe(3,6-DBCat)$_3$]$^{3-}$ ion formed at potentials near −1.0 V (Figure 3). The negative set of three oxidations correspond to the stepwise oxidation of the three catecholate ligands to semiquinone; the positive set corresponds to a series of coordinated semiquinone/benzoquinone oxidations. At potentials near +1.0 V, the benzoquinone ligands are subject to dissociation, particularly under the conditions of polar solvent and high electrolyte concentration necessary for the electrochemical experiment. As a result, negative scans fail to show a clear set of corresponding ligand reduction steps, and reductions of free 3,6-DBBQ are observed. Negative scans that begin near 0.0 V show three reversible reduction steps at −0.34 (80), −0.66 (150), and −0.88 (240) V that correspond to the SQ/Cat couples of the ligands, and a further irreversible reduction is observed at −1.2 V, which corresponds to the Fe(III)/Fe(II) reduction. The pattern of ligand-based oxidation steps is similar to that of the redox series of the Cr(SQ)$_3$ complexes.[10] The kinetic stability of Cr(III) permits observation of corresponding reduction steps without substantial benzoquinone dissociation in CH_2Cl_2 solution with a noncoordinating electrolyte. Reduction steps of Fe(3,6-DBSQ)$_3$ follow the pattern observed for the Fe(N-N)(3,6-DBSQ)(3,6-DBCat) complexes where two reversible ligand-based couples are observed at negative potentials, with an

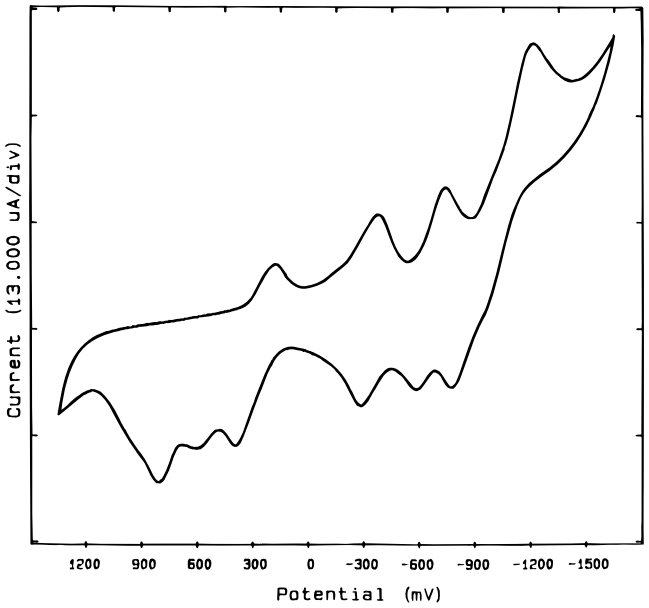

Figure 3. Cyclic voltammogram of Fe(3,6-DBSQ)$_3$ recorded in dichloromethane solution at a scan rate of 100 mV/s.

irreversible metal-based reduction appearing at potentials on the negative side of −1.0 V.[8]

Magnetism. Magnetic coupling between radical semiquinone ligands and high-spin Fe(III) has been investigated for members of the Fe(SQ)$_3$ series with semiquinone ligands derived from 9,10-phenanthrenequinone, 1,2-tetrachlorobenzoquinone, and 3,5-di-*tert*-butyl-1,2-benzoquinone.[4] Iron−SQ exchange is antiferromagnetic, and the magnitude of J_{Fe-SQ} has been found to be ligand dependent.[4,11] Fe(3,5-DBSQ)$_3$ has a temperature-independent magnetic moment of 2.9 μ_B associated with the $S = 1$ ground state, which results from strong coupling of the three metal dπ spins with the three radical ligands. Fe(Cl$_4$SQ)$_3$ and Fe(PhenSQ)$_3$ both show temperature-dependent magnetic behavior that results from weaker Fe−SQ exchange and magnetic moments below the $S = 1$ value at low temperature that result from intermolecular spin-coupling interactions. Structural studies have shown that semiquinone ligands of adjacent molecules pair in the solid state to provide a mechanism for intermolecular exchange. Magnetic characterization on the M(3,6-DBSQ)$_3$ series with M = Co, Al, and Ga and on Zn(tmeda)(3,6-DBSQ)$_2$ indicated that d-orbital-mediated exchange between radical SQ ligands through the dimagnetic Co(III) and Zn(II) ions was antiferromagnetic.[12] Exchange through the non-transition metal ions Al(III) and Ga(III) was ferromagnetic. Values for J_{SQ-SQ} for Co(3,6-DBSQ)$_3$ and Zn(tmeda)(3,6-DBSQ)$_2$ were −39.1 and −33.7 cm^{-1}, respectively, for $H = -2J_{SQ-SQ}[S_1 \cdot S_2 + S_1 \cdot S_3 + S_2 \cdot S_3]$. Attempts at modeling the changes in magnetic moment of Fe(Cl$_4$SQ)$_3$ and Fe(PhenSQ)$_3$ over the higher region of the temperature range, where intermolecular contributions are less significant, gave values for J_{Fe-SQ} of −60 and −100 cm^{-1}, respectively.[11] With the more recent information on SQ−SQ exchange, it becomes clear that interligand coupling must be considered in a suitable model for temperature-dependent changes in magnetism. Equation 1 has been derived as a first-order expression that includes the effects of both exchange interactions. Coupling between $S = {}^5/_2$ Fe(III) and three noninteracting $S = {}^1/_2$ radical ligands gives an $S = 1$ ground state, an $S = 2$ state $-4J_{Fe-SQ}$ higher in energy, a doubly degenerate $S = 2$ state at $-7J_{Fe-SQ}$, an $S = 3$ state at $-10J_{Fe-SQ}$, a doubly degenerate $S = 3$ state at $-13J_{Fe-SQ}$, and an $S = 4$ state at $-18J_{Fe-SQ}$. In the case where the three $S = {}^1/_2$ centers couple to give a doubly degenerate $S = {}^1/_2$ ground state at ${}^3/_2J_{SQ-SQ}$ and an $S = {}^3/_2$ state at $-{}^3/_2J_{SQ-SQ}$, these levels may be incorporated in the spin-coupling scheme to give eq 1. The change in spin-state energies is uncomplicated with shifts in only the degenerate $S = 2$ and $S = 3$ levels by factors of $3J_{SQ-SQ}$ above ground state. This expression has been fit to experimental data obtained on Fe(3,6-DBSQ)$_3$, and the results of this model are included in Figure 4. Agreement is reasonably good over the higher temperature range to 60 K; below 60 K, the effects of intermolecular exchange become important as the magnetic moment drops to 2.18 μ_B at 5 K. Values of J_{Fe-SQ} and J_{SQ-SQ} obtained from this fit are −139 and −235 cm^{-1}, respectively, for the spin Hamiltonian given in eq 2. Both exchange interactions are clearly antiferromagnetic, and the magnitude of SQ−SQ exchange is greater than that of the Fe−SQ exchange interaction. Since both exchange interactions are large and are of the same sign, they are correlated in the least-squares refinement with the experimental data, and their values are not comparable to coupling constants obtained from fits that use a single J to model either Fe−SQ or SQ−SQ independently. The J_{SQ-SQ}/J_{Fe-SQ} ratio of 1.7 is significant in showing that interligand exchange is nearly twice as great as iron−semiquinone exchange.

$$\chi_M = \frac{Ng^2\beta^2}{kT}\left[\frac{X}{Y}\right] \quad (1)$$

$$X = 2 + 10\exp(4J_{Fe-SQ}/kT) + 20\exp((7J_{Fe-SQ} - 3J_{SQ-SQ})/kT) + 28\exp(10J_{Fe-SQ}/kT) + 56\exp((13J_{Fe-SQ} - 3J_{SQ-SQ})/kT) + 60\exp(18J_{Fe-SQ}/kT)$$

$$Y = 3 + 5\exp(4J_{Fe-SQ}/kT) + 10\exp((7J_{Fe-SQ} - 3J_{SQ-SQ})/kT) + 7\exp(10J_{Fe-SQ}/kT) + 14\exp((13J_{Fe-SQ} - 3J_{SQ-SQ})/kT) + 9\exp(18J_{Fe-SQ}/kT)$$

$$H = -2J_{Fe-SQ}[S_{Fe}\cdot S_{SQ1} + S_{Fe}\cdot S_{SQ2} + S_{Fe}\cdot S_{SQ3}] - 2J_{SQ-SQ}[S_{SQ1}\cdot S_{SQ2} + S_{SQ1}\cdot S_{SQ3} + S_{SQ2}\cdot S_{SQ3}] \quad (2)$$

[Fe(3,6-DBSQ)$_2$(μ-OMe)]$_2$. Structure. The addition of nitrogen base ligands to Fe(3,6-DBSQ)$_3$ is accompanied by a change in color of the solution to dark blue as the Fe(N-N)-(3,6-DBSQ)(3,6-DBCat) product is formed by displacement of one quinone ligand.[8] Fe(3,6-DBSQ)$_3$ is soluble in alcohol, and a similar green/blue color change is observed. Related observations had been made for Fe(3,5-DBSQ)$_3$, Fe(Cl$_4$SQ)$_3$, and Fe(PhenSQ)$_3$, but no identifiable products were isolated. With Fe(3,6-DBSQ)$_3$ the product was obtained in crystalline form and characterized structurally. A view of the methoxide-bridged dimer [Fe(3,6-DBSQ)$_2$(μ-OMe)]$_2$ is shown in Figure 5; selected bond lengths and angles are listed in Table 5. The dimer is located about a crystallographic inversion center in the triclinic space group. Features of the quinone ligands are typically those of semiquinone with an average C−O length of 1.278(7) Å and slightly shorter ring C−C lengths at the C3−C4 and C5−C6 bonds. Bond lengths to the Fe are typical of Fe(III) with *trans* Fe−O$_{SQ}$ lengths to O2 and O4 averaging to 2.032(4) Å and *cis* Fe−O$_{SQ}$ lengths to O1 and O3 averaging to 2.024(5) Å. The difference between *cis* and *trans* lengths is less than that of [Fe(acac)$_2$(μ-OEt)]$_2$ where values of 2.025(4) and 1.997(4) Å were found with the shorter lengths to *cis* oxygens.[13] The

(11) Lynch, M. W.; Buchanan, R. M.; Pierpont, C. G.; Hendrickson, D. N. *Inorg. Chem.* **1981**, *20*, 1038.
(12) Lange, C. W.; Conklin, B. J.; Pierpont, C. G. *Inorg. Chem.* **1994**, *33*, 1276.

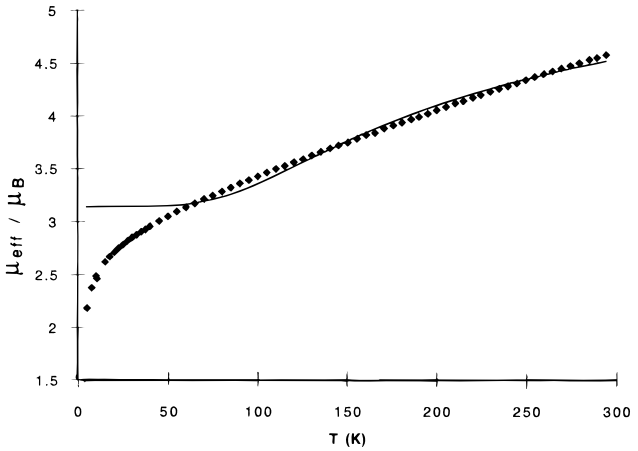

Figure 4. Changes in magnetic moment with temperature for Fe(3,6-DBSQ)$_3$. The solid line is the theoretical fit for a model including the effects of both Fe−SQ and SQ−SQ antiferromagnetic exchange calculated with a single g value of 2.12.

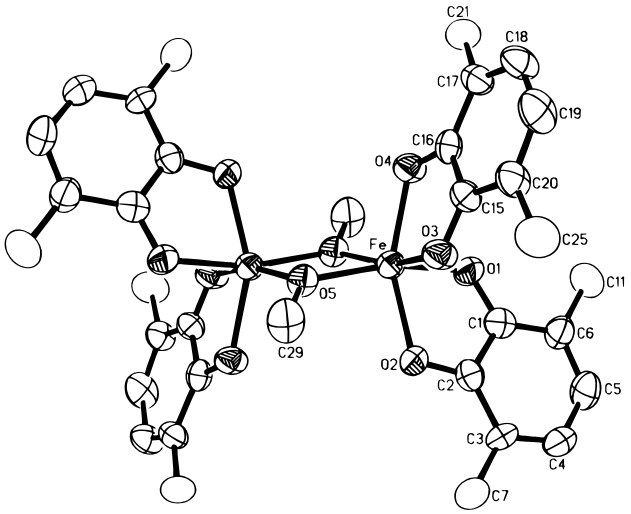

Figure 5. View of the centrosymmetric [Fe(3,6-DBSQ)$_2$(μ-OMe)]$_2$ dimer with *tert*-butyl methyl carbon atoms omitted.

Table 5. Selected Bond Lengths (Å) and Angles (deg) for [Fe(3,6-DBSQ)$_2$(μ-OMe)]$_2$

	Bond Lengths (Å)		
Fe−O1	2.022(6)	Fe−O2	2.034(4)
Fe−O3	2.026(5)	Fe−O4	2.030(4)
Fe−O5	1.972(5)	Fe−O5′	1.975(4)
	Fe- -Fe′ 3.093(1)		
O1−C1	1.276(8)	O2−C2	1.285(9)
C1−C2	1.465(13)	C1−C6	1.446(12)
C2−C3	1.420(9)	C3−C4	1.358(12)
C4−C5	1.427(14)	C5−C6	1.358(11)
O3−C15	1.269(7)	O4−C16	1.281(8)
C15−C16	1.473(12)	C15−C20	1.417(11)
C16−C17	1.447(9)	C17−C18	1.348(11)
C18−C19	1.433(13)	C19−C20	1.347(10)
	Angles (deg)		
O1−Fe−O2	77.6(2)	O3−Fe−O4	77.4(2)
O5−Fe−O5′	76.8(3)	Fe−O5−Fe′	103.2(3)

difference cannot be ascribed to an obvious *trans* influence since the Fe−O lengths to the bridging alkoxide oxygens are similar, with values of 1.973(5) Å for [Fe(3,6-DBSQ)$_2$(μ-OMe)]$_2$ and 1.979(4) Å for [Fe(acac)$_2$(μ-OEt)]$_2$. Further, features of the Fe_2O_2 rings for the two dimers are similar with imposed planarity, Fe−O−Fe angles of 103.2(3) and 103.6(3)° and Fe- -Fe separations of 3.093(1) and 3.116(1) Å.

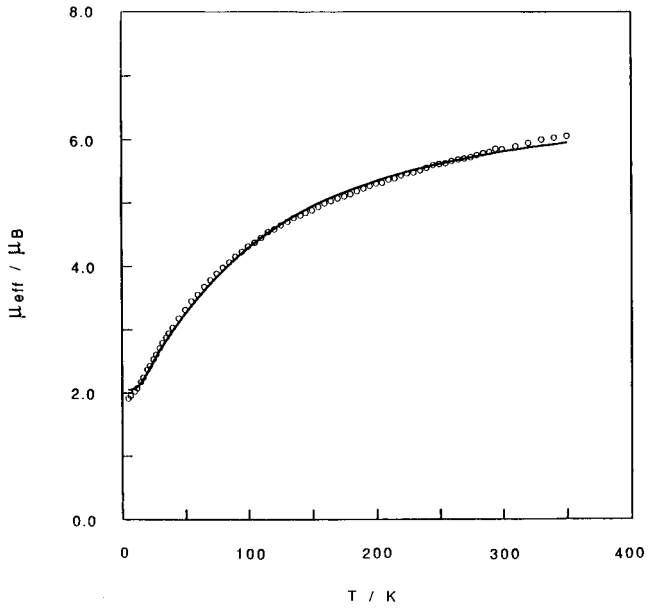

Figure 6. Temperature-dependent changes in magnetic moment for [Fe(3,6-DBSQ)$_2$(μ-OMe)]$_2$. The solid line is the theoretical fit for a model that includes only the effects of Fe−Fe superexchange.

Electrochemistry. Stepwise reductions of the four SQ ligands of the [Fe(3,6-DBSQ)$_2$(μ-OMe)]$_2$ dimer appear as quasireversible couples for negative CV scans that begin at +0.1 V (vs Fc^+/Fc). Ligand-based reductions appear at +0.62, −0.11, −0.52, and −0.79 V. An irreversible one-electron reduction appears at a more negative potential that corresponds to the Fe(III/II) reduction of one metal ion of the dimer. Positive scans from 0.0 V show oxidations at +0.45, +0.80, and +1.48 V, but without coupled reductions. Here also oxidation of the semiquinone ligands to 3,6-DBBQ leads to dissociation and irreversible electrochemical activity at positive potentials.

Magnetism. Magnetic measurements made on [Fe(3,6-DBSQ)$_2$(μ-OMe)]$_2$ show strong temperature dependence with magnetic moment *per dimer* dropping from a value of 6.04 μ_B at 350 K to 1.91 μ_B at 5 K (Figure 6). Intramolecular exchange interactions include both Fe−SQ and SQ−SQ exchange within Fe(3,6-DBSQ)$_2$ units, as well as Fe−Fe coupling between bridged units. A theoretical expression that includes the effects of all three coupling interactions could be derived, but a less complicated model based on the assumption that all three coupling interactions are antiferromagnetic and that the magnitude of J_{Fe-SQ} is greater than that of J_{Fe-Fe} was used to give reasonably good agreement with experimental measurements. Justification for these assumptions comes from the value of J_{Fe-SQ} for Fe(3,6-DBSQ)$_3$ and the results of magnetic measurements on alkoxide-bridged dimers of Fe(III) which generally have J_{Fe-Fe} coupling constants that are less than −20 cm^{-1}.[13,14] A dimer consisting of coupled $S = {}^3/_2$ Fe(SQ)$_2$ units that arise from strong Fe−SQ and SQ−SQ exchange was used to give the theoretical curve shown in Figure 6. Equation 3 was used

$$\chi_M = (2Ng^2\beta^2/kT)[(\exp(2J_{Fe-Fe}/kT) + 5\exp(6J_{Fe-Fe}/kT) + 14\exp(12J_{Fe-Fe}/kT))/(1 + 3\exp(2J_{Fe-Fe}/kT) + 5\exp(6J_{Fe-Fe}/kT) + 14\exp(12J_{Fe-Fe}/kT))] \quad (3)$$

to fit the experimental data. This expression had been derived previously to model the exchange interactions in alkoxo-bridged

(13) Chiari, B.; Piovesana, O.; Tarantelli, T.; Zanazzi, P. F. *Inorg. Chem.* **1984**, *23*, 3398.
(14) Walker, J. D.; Poli, R. *Inorg. Chem.* **1990**, *29*, 756.

Cr(III) dimers with the Heisenberg Hamiltonian defined as $H = -2J_{Fe-Fe}(S_1 \cdot S_2)$.[15] The fit shown in Figure 6 was obtained for $J_{Fe-Fe} = -22.5$ cm^{-1}, $g = 2.37$, TIP $= 6.1 \times 10^{-4}$ emu/mol, and a P value of 0.085 for a low-level paramagnetic impurity. The value for J_{Fe-Fe} is at the higher end of the range for alkoxo-bridged Fe(III) dimers. Exchange between the $S = {}^5/_2$ centers of $[Fe(acac)_2(\mu\text{-OEt})]_2$ is -11.0 cm^{-1}, while for the $[FeCl_3(\mu\text{-OEt})]_2$ dimer containing five-coordinate metal ions J_{Fe-Fe} is -24.6 cm^{-1}.[13,14]

Discussion

Magnetic exchange between paramagnetic metal ions and radical semiquinone ligands has been a subject of study for nearly 20 years.[2,16] As a general observation, M−SQ coupling is strong and antiferromagnetic for unpaired dπ metal electrons. Members of the $Cr(SQ)_3$ series are very nearly diamagnetic at room temperature, and M−SQ exchange for Ni(bpy)(3,5-DBSQ)$_2$, where metal spins are in dσ orbitals, is weak with $J_{Ni-SQ} = 0.7$ cm^{-1}.[11] High-spin Fe(III), with spins in both dπ and dσ orbitals, couples most strongly with SQ ligands through dπ−SQ interactions giving, in the limit of strong, antiferromagnetic exchange ($J_{Fe-SQ} > -200$ cm^{-1}), an $S = 1$ ground state. Magnetic characterization on Fe(3,5-DBSQ)$_3$ has shown that this complex remains in the $S = 1$ state at room temperature with little population of higher order spin states. High-field Mossbauer spectra recorded on both Fe(3,5-DBSQ)$_3$ and Fe(PhenSQ)$_3$ show that there are no changes in charge distribution or shifts in metal ion spin state down to 5 K, and we assume in the present analysis that this also applies to Fe(3,6-DBSQ)$_3$.[6] In cases where population of higher order spin states that result from Fe−SQ coupling give rise to a temperature-dependent magnetic moment, it had been of interest to estimate J_{Fe-SQ} by fitting the experimental measurements to the theoretical expression for magnetic susceptibility derived from a model consisting of three noninteracting $S = {}^1/_2$ radical centers coupled to an $S = {}^5/_2$ core.[11] A model of this type has been used to simulate the magnetic properties of a tetrametallic system consisting of a Mn^{2+} core linked to three equivalent Cu^{2+} ions.[17] When the model was applied to Fe(Cl$_4$SQ)$_3$ and Fe(PhenSQ)$_3$, approximate values of J_{Fe-SQ} could be obtained, -60 and -100 cm^{-1}, but the quality of the fit was poor. Gudel used a two-J model to describe the magnetic properties of $[Cr\{Cr(en)_2(\mu\text{-}OH)_2\}_3]^{6+}$.[18] In this case, an improved fit was obtained for the triangular ion by including the effects of Cr−Cr exchange along edges as well as edge−core exchange, but edge−edge coupling was relatively small. The use of a two-J model to account for the temperature-dependent magnetic properties of members of the Fe(SQ)$_3$ series provides an improved fit for data above 100 K. Low-temperature magnetic data drop below the limiting $S = 1$ value due to intermolecular exchange.[4] X-ray structure determinations have shown that there are close intermolecular contacts, and high-field Mossbauer measurements verify that the metal ions of these complexes are normal $S = {}^5/_2$ Fe(III).[6] Nonlinear least-squares refinement of the model, including the effects of both Fe−SQ and SQ−SQ coupling, was carried out using the experimental data obtained for Fe(3,6-DBSQ)$_3$ and the magnetic measurements on Fe(PhenSQ)$_3$ and Fe(Cl$_4$SQ)$_3$ reported earlier.[4] In all three cases, J_{Fe-SQ} and J_{SQ-SQ} were found to be strongly correlated. Upon refinement, both coupling constants were observed to increase together in magnitude to unreasonably large, negative values. However, while the J values obtained from refinement are meaningless, in all three cases they both are indicative of antiferromagnetic exchange. Further, in each case J_{SQ-SQ} refined to a value that is approximately twice the value of J_{Fe-SQ}. Both spin-coupling interactions involve contributions from metal dπ levels, direct spin coupling for Fe−SQ exchange, or as a medium for superexchange between ligand π spins, and this contributes to the strong correlation between J values. While it has not been possible to determine the magnitude of the two exchange interactions, it is clear that both are antiferromagnetic, that a single J_{Fe-SQ} does not provide an adequate fit to the experimental magnetic data for all three Fe(SQ)$_3$ complexes, and that SQ−SQ exchange is substantially stronger than Fe−SQ exchange.

Acknowledgment. We thank Professor Gordon Yee for helpful comments concerning the interpretation of magnetic data. Support for this research was provided by the National Science Foundation through Grant CHE 90-23636 and the Egyptian Ministry of Science in the form of a Graduate Fellowship for A.S.A.

Supporting Information Available: Tables giving crystal data and details of the structure determination, atomic coordinates, anisotropic thermal parameters, hydrogen atom locations, and bond lengths and angles for Fe(3,6-DBSQ)$_3$ and $[Fe(3,6\text{-DBSQ})_2(\mu\text{-OMe})]_2$ (26 pages). Ordering information is given on any current masthead page.

IC950595C

(15) Hodgson, D. J. *Prog. Inorg. Chem.* **1975**, *19*, 186.
(16) Dei, A.; Gatteschi, D. *Inorg. Chim. Acta* **1992**, *198*−*200*, 813.
(17) Lloret, F.; Journaux, Y.; Julve, M. *Inorg. Chem.* **1990**, *29*, 3967.
(18) Gudel, H.; Hauser, U. *Inorg. Chem.* **1980**, *19*, 1325.